Regular Article

PHYSICAL CHEMISTRY RESEARCH
Published by the
Iranian Chemical Society
www.physchemres.org
info@physchemres.org

Phys. Chem. Res., Vol. 11, No. 2, 391-408, June 2023
DOI: 10.22036/pcr.2022.343322.2108

A Comparative Study Through DFT Investigation and Molecular Docking Studies of Potential Dietary Phytochemicals Against Cancer Target-DNA Topoisomerase III

P. Sarkar, V. Srivastava and M. Guin*

Department of Chemistry and Biochemistry, School of Basic Sciences and Research, Sharda University, Greater Noida 201310, India

(Received 20 May 2022, Accepted 5 July 2022)

The objective of this work is to understand the potential of small natural dietary phytochemicals as inhibitors of cancer target enzymes. In this regard, Density Functional Theory (DFT) study and molecular docking analysis of five potential food phytochemicals *e.g.* crocetin (Cr), ellagic acid s (Ea), fernesiferol (Fe), dillapiole (Di), shogaol (Sh) have been performed. Also, two FDA approved anticancer drugs afinator and azacitidine were studied along with these molecules for comparison. The preliminary computational studies indicate the strength of these phytochemicals to bind strongly with the cancer target-DNA topoisomerase III beta. DFT studies are performed to understand the electronic structure and probable binding sites of these phytochemicals. Among the chosen five bioactive molecules, Cr is found to have the highest binding energy of -42.43 kcal mol^{-1} with DNA topoisomerase III beta. Although afinator drug has higher binding energy (-44.12 kcal mol^{-1}) than Cr, it has many side effects. Cr, being a natural compound with similar level of binding energy and less toxicity, is more appealing as a drug. The DFT analysis indicates Cr with the lowest ionization energy, as the most reactive molecule.

Keywords: Dietary phytochemicals, DFT, MEP, Molecular docking, DNA topoisomerase III beta

INTRODUCTION

DNA topoisomerase III beta controls and alters the topological condition of DNA during transcription. This enzyme catalyzes the transient breaking and rejoining of a single strand of DNA which allows the strands to pass through one another, thus relaxing the supercoils and altering the topology of DNA. This enzyme is also responsible for the formation of RNA loop structures [1]. Many product-derived agents, such as camptothecin, anthracycline, and podophyllotoxin drugs, have been broadly used in the treatment of many types of cancer. Selective targeting of the topoisomerase enzymes for cancer treatment continues to be a highly active area in basic and clinical research [2]. Despite selective targeting, some drugs become resistant to cancer cells. Additionally, chemotherapy leads to severe toxicity and side effects that causes extreme pain during the recovery process [3].

Computational studies can screen the potential applicability of various phytochemicals that can later be validated using laboratory-based experiments. Computational techniques such as molecular docking and density functional theory (DFT) studies considering the highest occupied molecular orbital (HUMO), lowest unoccupied molecular orbital (LUMO), and molecular electrostatic potential (MEP) are mostly preferred by researchers [4,5]. Molecular docking is an established *in silico* structure-based method widely used in drug discovery. Docking enables the identification of novel compounds of therapeutic interest, predicting ligand-target interactions at the molecular level, or delineating structure-activity relationships (SAR), without knowing a priori the chemical structure of the target modulators. Although it was originally developed to understand the mechanisms of molecular recognition between small and large molecules, their uses and applications in drug discovery have heavily

*Corresponding author. E-mail: mridula.guin@sharda.ac.in

changed over the last few years [3,6]. This process is generally accomplished by first predicting the molecular orientation of a ligand within a receptor, and then estimating their complementarity through the use of a scoring function [7,8].

The rapid growth and advancement in the computational field because of the availability of cheaper and faster computers and better algorithm propels the field of computational research. The advent of DFT helps in interpreting ambiguous or conflicting experimental results. It became an extremely popular code for predicting variety of molecular properties. The reactivity descriptors under the conceptual DFT framework are extensively studied by many research groups and are found to be extremely helpful in understanding the reactivity behavior of molecular systems [9-13].

Chemotherapy using synthetic drugs having high molecular weight may often lead to severe side effects including drug resistance against cancer cells [3]. To overcome such unwanted effects, a suitable and specific approach is required. In this regard, small natural bioactive substances, found in various plant species play an important role [8-10]. Natural phytochemicals like crocetin (Cr), ellagic acid (Ea), fernesiferol (Fe), dillapiole (Di), and shogaol (Sh) are present in various plants like *crocus sativus, syzygium aromaticum, foeniculum vulgare, and ginger officinale* were tried against DNA topoisomerase III beta, one of the potential cancer target. These natural compounds are consumed as food ingredients. Therefore, taking these non-toxic compounds as drugs would be highly beneficial in chemotherapy [14]. In this context we have done a preliminary computational study using DFT and molecular docking approach. The structures of these compounds were initially optimized using various DFT investigations and then later molecular docking procedures were applied to understand the potential inhibitory sites on the DNA topoisomerase III beta and also their role as strong inhibitors [15]. Density Functional Theory (DFT) studies are performed to determine the electronic structure of these phytochemicals to understand their chemical reactivity and relative stability. The molecular electrostatic potential map of these compounds has been determined to identify the electrophilic and nucleophilic sites of interaction.

METHODS

Density Functional Theory (DFT) Study

Elucidation of the electronic structure of the molecules is performed through Density Functional Theory (DFT) calculations using Gaussian 16 program package [16]. DFT calculations using hybrid functionals deliver excellent computational accuracy with limited computational cost. The geometry optimization was carried out by B3LYP functional with 6-31++G(d,p) basis set. B3LYP exchange-correlation function with 6-31++G(d,p) basis set is carried out as it is the choice for medium to large systems offering the right balance of accuracy with efficiency. The convergence criteria were maintained at the default level without any constraint on the geometry. The analytic vibrational frequency of the global minima structure is computed at the same level to confirm the geometry to be minima on the potential energy surface. The energy of HOMO and LUMO is determined to understand the chemical reactivity of the compound.[17-19]Global reactivity descriptors in the framework of conceptual density functional theory (CDFT) have been computed. Moreover, the molecular electrostatic potential of the compound is calculated from the electron density to predict its reactive sites [17].

Molecular Docking Procedure

PatchDock server-Bioinfo 3D, a molecular docking algorithm [7] based on the shape complementarity principle is applied to carry out molecular docking studies on the selected compounds. The main role is to understand the binding pattern and the different types of interaction of these compounds with the amino acid present in the enzyme, human DNA topoisomerase III beta. The enzyme was selected as a cancer target due to its potential role in the DNA replication process. It was downloaded from Protein Data Bank as PDB files (PDB id 5GVC). 5GVC was chosen with a resolution of 2.44 A, R-Value free of 0.229, R-Value work of 0.182, and R-Value observed of 0.184, https://www.rcsb.org/structure/5GVC. Water molecules, cofactors, and the inhibitors already attached to the enzyme were removed so that they do not cause any interference during the docking study. We performed structure-based molecular docking as the structure of both the targets and the ligands were known to us.

All the ligands (dietary bioactive compounds) were downloaded from the Pub Chem database (https://pubchem.ncbi.nlm.nih.gov/) in SDF format. All structures were optimized using DFT calculation. The optimized structures from DFT calculations were used as the initial ligand in the docking procedure. After that, the ligands were converted to PDB format with the help of an online SMILES translator and the structure file generator built by the CADD Group's Chemoinformatics Tools and User Services, NIH. Every ligand (bioactive compound) and desired protein were selected one by one using Patch Dock web server and a docking experiment was done.

Patch Dock web server works in an online mode and predicts all the docking analysis based on structure-based rigid docking calculation. The output files were generated as various docking poses depicting different types of non-covalent and non-bonding interaction which was then analyzed in detail for molecular docking analysis. Patch Dock molecular docking web server predicts one thousand different binding interactions between protein and ligand with highest to lowest order from top to bottom in the form of solution no. FireDock then filters top ten results after fine refinement and transformation and sorted these solutions according to global energy, the binding energy of each solution. Each solution represents one best molecular docking binding pose (strongest interaction) out of several others. All the docking results were then visualized using BIOVIA discovery studio visualizer. Similarly, two FDA-approved standard anticancer drugs afinator and azacitidine were also investigated for the sake of comparison and as a positive control for the docking experiment.

RESULTS AND DISCUSSIONS

Density Functional Theory (DFT) Study

Geometry, energy, and frontier molecular orbital analysis. The optimized geometry of the molecules along with their atom numbering is shown in Fig. 1. Selected structural parameters and thermodynamic parameters such as free energy, enthalpy, electronic energy, and dipole moment of the molecules calculated at B3LYP/6-31++G(d,p) level are listed in Table 1 and Table 2, respectively. Spectroscopic

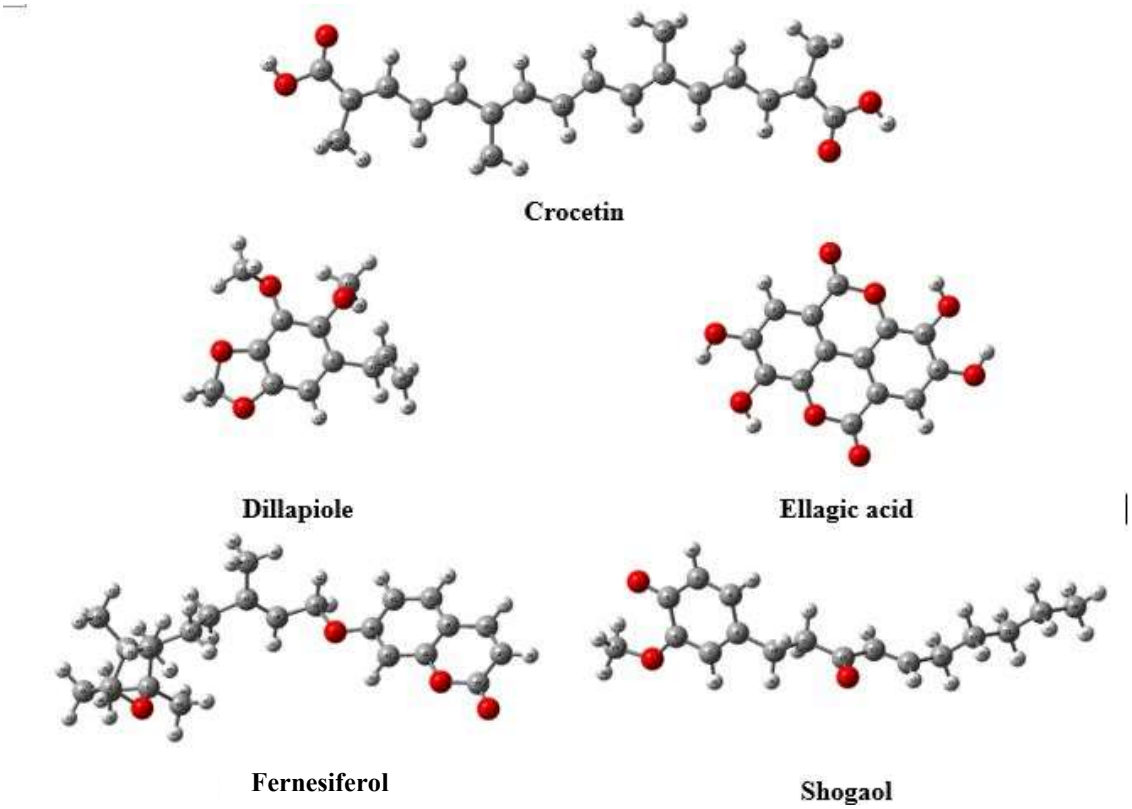

Fig. 1. Optimized geometry of the studied compounds. Colour code: Red: O; Grey: C; and White: H.

Table 1. Selected Structural Parameters of the Investigated Compounds at B3LYP/6-31++G(d,p) Level

Bond parameter	Bond lengths (Å)	Bond angle parameter	Bond angle (°)
Crocetin			
H47–O1	0.971	C23–O1–H47	106.2
C23–O1	1.364	O1–C23–O3	121.0
C23–O3	1.221	C19–C23–O1	112.4
C23–C19	1.483	C19–C23–O3	126.5
C19–C17	1.362	C24–O2–H48	106.3
C19–C21	1.506	C20–C24–O2	112.4
C17–H39	1.088	C23–C19–C21	118.3
C21–H43	1.091	C21–C19–C17	125.8
C21–H41	1.095	C23–C19–C17	115.9
C17–C15	1.438	C17–C15–C9	121.9
C15–H37	1.086	C19–C17–C15	127.4
C15–C9	1.365	C15–C9–C5	126.6
C9–H27	1.090	C9–C5–C13	118.6
C9–C5	1.445	C9–C5–C7	117.8
C5–C13	1.509	C13–C5–C7	123.5
C13–H33	1.096	C5–C7–C11	127.9
C13–H32	1.090	C7–C11–C12	123.3
C5–C7	1.374	C11–C12–C8	123.3
C7–H25	1.090	C12–C8–C6	127.9
C7–C11	1.431	C8–C6–C14	123.5
C11–H29	1.088	C8–C6–C10	117.8
C11–C12	1.369	C14–C6–C10	118.6
C13–H33	1.088	C6–C10–C16	126.6
C12–C8	1.431	C10–C16–C18	121.9
C8–H26	1.090	C16–C18–C20	127.4
C8–C6	1.374	C18–C20–C22	125.8
C6–C14	1.509	C18–C20–C24	115.9
C14–H34	1.096	C24–C20–C22	118.3
C14–H36	1.090	C20–C24–O4	126.5
C6–C10	1.446	O2–C24–O4	121.0
C10–H28	1.090		
C10–C16	1.365		
C16–H38	1.086		
C16–C18	1.438		
C18–H40	1.088		
C18–C20	1.362		
C20–C22	1.506		
C20–C24	1.483		
C22–H46	1.095		
C22–H45	1.091		
C24–O2	1.364		
C24–O4	1.221		
O2–H48	0.971		
Ellagic acid			
1.359	C7–O14–H26	109.4	
0.969	C8–C7–O14	119.8	
1.361	C7–C8–O13	117.4	
0.970	C8–O13–H25	109.8	
1.375	C8–C9–O10	117.9	
1.409	C9–O10–C11	122.9	
1.206	O10–C11–O12	116.83	
1.359	C20–O21–H27	109.5	
0.969	C19–C20–O21	119.8	
1.361	C20–C19–O22	117.4	
0.970	C19–O22–H28	109.8	
1.375	C19–C18–O17	117.9	
1.409	C18–O17–C15	122.9	
1.206	O17–C15–O16	116.8	
1.412			
1.391			
1.392			
1.407			
1.401			
1.394			
1.083			
1.472			
1.392			
1.425			
1.406			
1.472			
1.401			
1.394			
1.412			
1.391			
1.084			
Dillapiole			
C9–O4	1.369	C15–O4–C9	116.1
C15–O4	1.436	C6–C9–O4	123.9
C8–O3	1.379	C8–C9–O4	119.5
C14–O3	1.435	C8–C9–O3	119.5
C6–O1	1.382	C5–C8–O3	118.6
C12–O1	1.437	C8–O3–C14	115.8
C12–O2	1.429	C9–C6–O1	128.6
C7–O2	1.383	C6–O1–C12	104.2
C5–C11	1.520	O1–C12–O2	107.3
C11–C13	1.511	C12–O2–C7	104.8
C13–C16	1.336	C6–C7–O2	109.0
C9–C6	1.388	C10–C7–O2	128.5
C6–C7	1.390	C7–C6–C9	121.5
C7–C10	1.379	C6–C9–C8	116.5
C10–C5	1.412	C9–C8–C5	121.8
C5–C8	1.404	C8–C5–C10	119.9
C8–C9	1.419	C5–C10–C7	117.6
C15–H28	1.096	C10–C7–C6	122.4
C15–H26	1.091	C5–C11–C13	112.7
C15–H27	1.094	C11–C13–C16	124.8
C12–H20	1.091	C8–C5–C11	120.2
C12–H21	1.100		
C10–H17	1.084		
C14–H24	1.098		
C14–H23	1.092		
C14–H25	1.093		
C11–H19	1.096		
C11–H18	1.095		
C13–H22	1.089		

Table 1. Continued

C16–H29	1.086		
C16–H30	1.088		
Fernesiferol			
C28–O4	1.211	O4–C28–C27	126.2
C28–O3	1.398	O4–C28–O3	117.5
C27–C28	1.457	C28–C27–H58	115.7
C26–C27	1.358	O3–C23–C21	117.2
C26–C25	1.437	O2–C20–C21	115.4
C25–C23	1.413	C20–O2–C19	119.2
C23–O3	1.367	O2–C19–C18	107.7
C23–C21	1.388	O2–C20–C22	124.3
C21–C20	1.401	C19–C18–C16	127.6
C20–C22	1.411	C18–C16–C17	124.8
C22–C24	1.389	C18–C16–C15	119.7
C24–C25	1.405	C16–C15–C11	113.5
C20–O2	1.358	C15–C11–C7	113.9
C19–O2	1.444	C11–C7–C6	117.2
C19–C18	1.496	C11–C7–C5	115.3
C18–C16	1.345	C7–C6–C14	119.6
C16–C17	1.510	C7–C6–C9	107.8
C16–C15	1.518	C7–C6–O1	102.6
C15–C11	1.546	C9–C6–O1	101.3
C11–C7	1.540	C10–C8–O1	102.3
C7–C6	1.578	C5–C8–O1	101.6
C6–C14	1.516	C6–O1–C8	97.4
C6–C9	1.554	C6–C9–C10	101.8
C9–C10	1.554	C9–C10–C8	101.1
C10–C8	1.544	C10–C8–C5	113.6
C8–C5	1.557	C6–C7–C5	101.3
C7–C5	1.588	C7–C5–C8	99.8
C6–O1	1.451	C7–C5–C13	112.1
C8–O1	1.438	C8–C5–C12	107.3
C5–C13	1.536	C12–C5–C13	108.5
C5–C12	1.543		
Shogaol			
C6–O2	1.260	O2–C6–C9	121.6
C6–C4	1.469	O2–C6–C4	122.6
C4–O1	1.343	C6–C4–O1	124.5
O1–C14	1.441	C4–O1–C14	123.6
C4–C7	1.401	C7–C4–O1	115.3
C7–C5	1.394	C5–C10–C11	112.3
C5–C8	1.428	C10–C11–C12	113.6
C8–C9	1.369	C11–C12–C13	115.8
C9–C6	1.450	C12–C13–C15	122.0
C5–C10	1.509	C13–C15–C16	125.7
C10–C11	1.538	C15–C16–C17	112.8
C11–C12	1.525	C16–C17–C18	112.9
C12–C13	1.487	C17–C18–C19	113.4
C12–O3	1.225	C18–C19–C20	113.2
C13–C15	1.343		
C15–C16	1.497		
C16–C17	1.543		
C17–C18	1.534		
C18–C19	1.534		
C19–C20	1.533		

characterization using NMR, mass, IR, UV of crocetin derivatives [20], ellagic acid [21,22], ferulic acid [23], dillapiole [24,25], and shogaol [26] have been reported by many researchers. Our computed results match closely with the reported structural data. In addition, various electronic properties for example energy of the highest occupied molecular orbital (EHOMO) and lowest unoccupied molecular orbital (ELUMO), Energy difference (Egap) between HOMO and LUMO orbitals are also computed. In accordance with Koopman's theorem [27], ionization potential (I) and electron affinity (A) of a molecule is related to EHOMO and ELUMO respectively. HOMO and LUMO are also known as frontier orbitals and these orbitals are responsible for the reactivity and stability of a molecule. Various other reactivity parameters such as global hardness (h), softness (S), electronegativity (c), chemical potential (m) and electrophilicity index (w), electrodonating power (w-), electroaccepting power (w+) of the compounds are calculated. The energy of HOMO indicates how easily a molecule can donate its electron while the energy of LUMO characterizes the electron accepting ability of a molecule. [28,29] High value of EHOMO means easy donation of electrons and vice versa. The HOMO and LUMO values along with global reactivity descriptors are listed in Table 3. It is evident from the results in Table 2, that Cr has the highest HOMO energy (-5.427 eV) and it is the best electron donor among the studied molecules. The molecule Sh with LUMO energy of -3.486 eV is the best electron acceptor among these molecules.

The calculated 3D plots of frontier orbitals HOMO and LUMO with the energy gap are shown in Fig. 2. The computed energy gap determines whether the molecules are stable and polarized. Various literature reports correlate these values with the bioactivity of a compound as well as binding ability with a target molecule [17]. A stronger interaction is facilitated when the target molecule with high HOMO energy acts as an electron donor with the interacting molecule as an acceptor with lower LUMO energy. The global reactivity descriptors explain the chemical reactivity and kinetic stability of the compound. Ionization energy is the energy needed to remove an electron from a molecule. The higher the value of ionization energy, the higher the stability or chemical inertness whereas low ionization energy is related

Table 2. Thermodynamic Parameters of the Investigated Compounds Calculated at B3LYP/6-31++G(d,p) Level

Compound	Free energy (Hartree)	Enthalpy (Hartree)	Electronic energy (Hartree)	Dipole moment (Debye)
Cr	-1077.200541	-1077.111106	-1077.139052	0.000300
Ea	-1138.850977	-1138.790090	-1138.807833	0.004758
Fe	-1233.142145	-1233.053621	-1233.081244	8.970976
Di	-766.365693	-766.304231	-766.321178	1.665932
Sh	-887.041424	-886.961599	-886.984652	4.199889

Table 3. FMO Energy Parameters and Global Ractivity Descriptors of the Compound

Parameters	Cr	Di	Ea	Fe	Sh
HOMO (eV)	-5.427	-5.769	-6.437	-6.312	-5.694
LUMO (eV)	-3.026	-0.382	-2.472	-1.961	-3.486
ΔE = (LUMO-HOMO) (eV)	2.401	5.387	3.965	4.351	2.208
I = -E(HOMO) (eV)	5.427	5.769	6.437	6.312	5.694
A = -E(LUMO) (eV)	3.026	0.382	2.472	1.961	3.486
$\chi = (I + A)/2$ (eV)	4.226	3.075	4.454	4.136	4.590
$\mu = -\chi$ (eV)	-4.226	-3.075	-4.454	-4.136	-4.590
$\eta = (I - A)/2$ (eV)	2.401	2.693	3.965	2.175	1.104
$S = 1/\eta$ (eV)	0.416	0.371	0.252	0.459	0.906
$\omega = \mu^2/2\ \eta$ (eV)	3.719	1.755	2.502	3.932	9.542
$\omega^- = (3I + A)^2/16(I - A)$	9.703	3.630	7.479	6.273	11.975
$\omega^+ = (I + 3A)^2/16(I - A)$	5.478	0.554	3.025	2.136	7.385

to the high reactivity of the molecule. Among all molecules, Cr is having the lowest ionization energy, suggesting it as the most reactive molecule. The energy released when an electron is added to a neutral molecule is called electron affinity. A molecule having high electron affinity can accept electrons easily. According to the computed data, the molecule Sh has the highest electron affinity. Various other global chemical reactivity descriptors are also calculated. These parameters are closely associated with the structural configuration of the molecule. The chemical potential is the escaping tendency of an electron and is related to electronegativity. Among the studied molecules, Di is the least stable and reactive molecule according to the chemical potential data. Sh has the highest electronegativity among all the molecules. The hardness and softness of a molecular system play a major role in understanding the reactive behavior of a molecule. Soft molecules have a low energy gap and they are easily polarizable compared to hard molecules. The higher the value of the global hardness, the lower the reactivity while the higher value of global softness indicates higher reactivity. Ea and Di are the molecules with the highest values of hardness and softness respectively. Electrophilicity signifies the stability of a molecule in case it is saturated with electrons from an external source. The lower value of ω suggests a reactive nucleophile whilst a higher value indicates a good electrophile. In the present study, Di

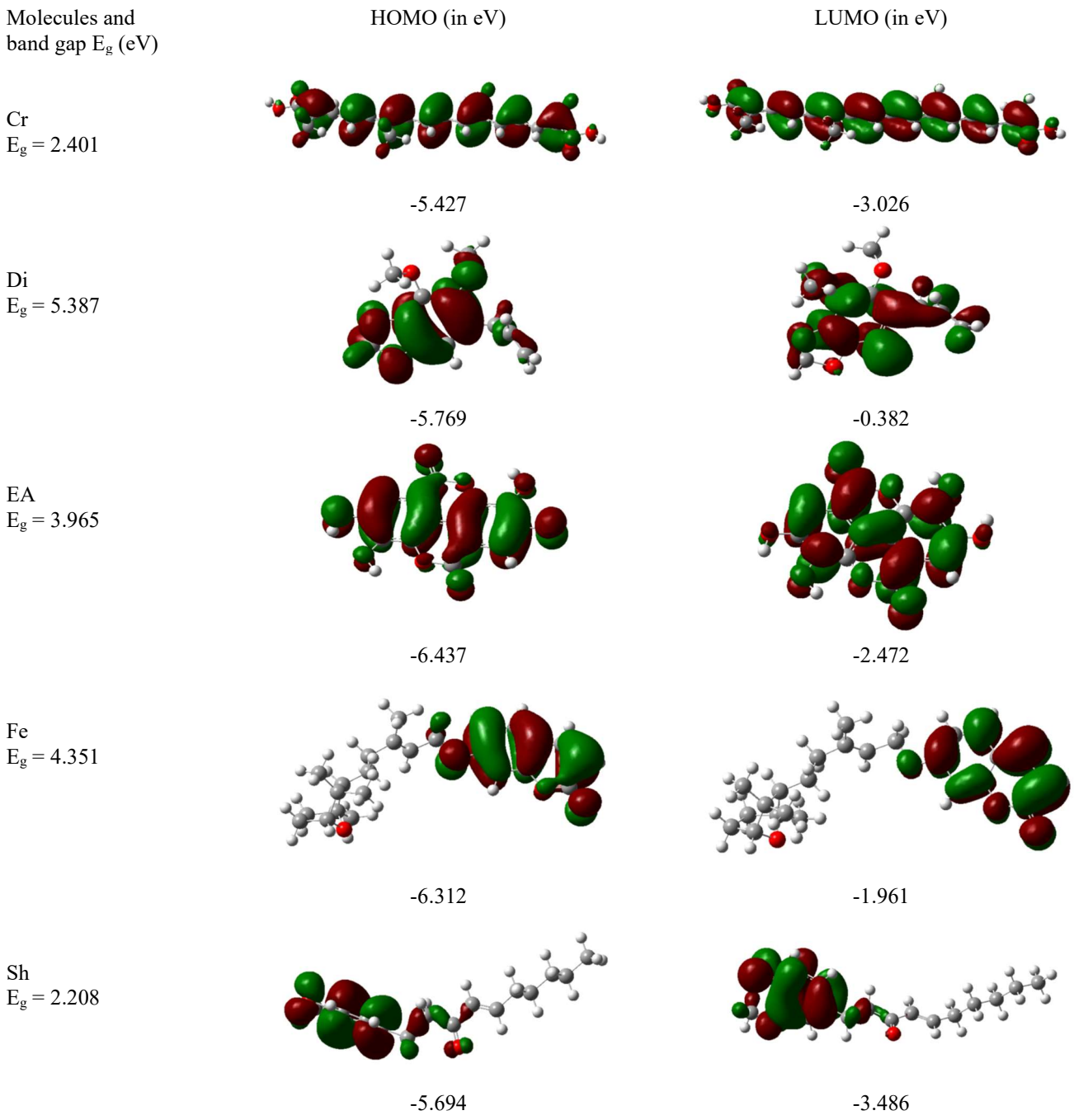

Fig. 2. HOMO, LUMO plots and band gap of the molecules were calculated at B3LYP/6-31++G(d,p) level.

is the best nucleophile with the lowest electrophilicity and Sh is the best electrophile with the highest electrophilicity.

The molecular electrostatic potential (MEP) of the compounds is computed using the electron density of the molecules and displayed in Fig. 3 with their color-coded scale. The MEP diagram describes the charge distribution in the molecule and predicts the electrophilic and nucleophilic active sites of the complex based on the electron density [30].

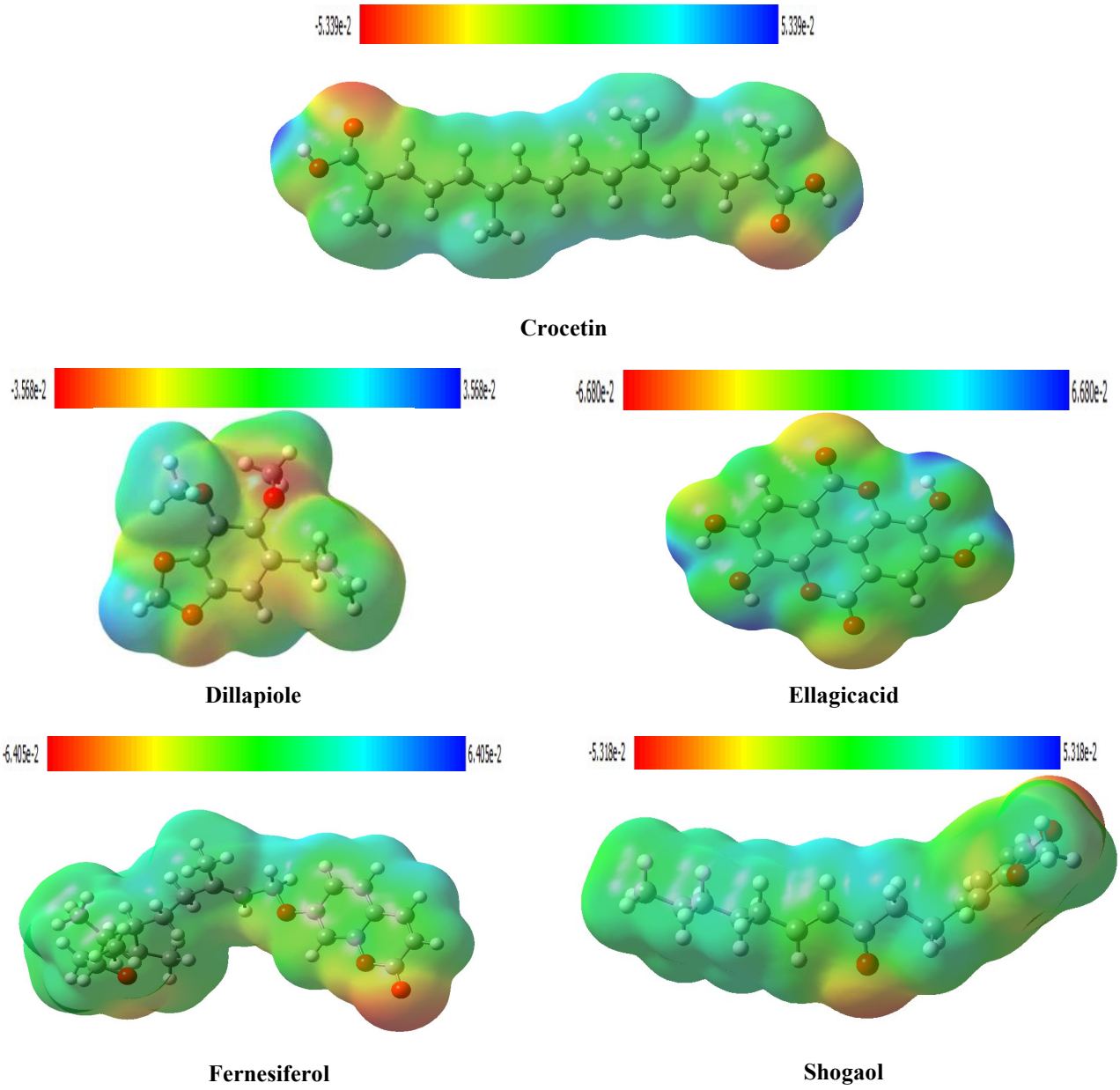

Fig. 3. Molecular electrostatic potential map of the investigated compounds.

The increasing order of electrostatic potential is indicated in the colour scale from red to blue. The region with green colour is the region with zero potential. In the MEP map, the oxygen atoms in the moiety are observed as the strong electrophilic region with bright red to orange colour. These sites are responsible for the electrophilic reactivity of the compound. While the regions with blue colour are associated with positive electron density for nucleophilic reactivity.

Molecular Docking Procedure

All the five bioactive molecules namely ellagic acid, dilapiole, fernesiferol, shogaol, and crocetin were docked one by one to the active sites of the enzyme, DNA Topoisomerase III beta. Among 1000 different modes of binding, the best

10 possible modes of interaction were screened and selected using PatchDock molecular docking software. Additionally, we have performed molecular docking study of two FDA-approved drugs Afinator and Azacitidine against DNA topoisomerase III beta. The binding results were shown in the form of global energy in Table 4. From Table 4, it can be seen that Di has the highest global energy in solution 1 (-32.36 kcal mol^{-1}), Ea has global energy of -36.71 kcal mol^{-1} in solution 3, Fe with -41.25 kcal mol^{-1} in solution 3, Sh with -36.16 kcal mol^{-1} in solution 1. Cr with global energy of -42.43 kcal mol^{-1} which is the highest among all the five plant bioactive molecules chosen for the study. The highest global energy of Cr (crocetin) may be due to the long, linear structure of the molecule that allows it to interact strongly with the amino acid residues of the enzyme.

Additionally, from the molecular docking results, it may be understood that crocetin not only has the highest global energy of binding but the results also depict that it has the highest repulsive and attractive van der Waals forces along with the highest solvation energy. These forces are equally important for the study as these contribute to the total energy in the form of overall binding energy released when crocetin binds strongly with the target enzyme. Different types of molecular interactions between these five phytochemicals with DNA Topoisomerase III beta are listed in Table 5. Atomic contact energy is defined as the energy of replacing a protein-atom/water contact, with a protein-atom/protein-atom contact. The results in Table 5 depict that crocetin has the highest atomic contact energies along with the highest attractive and repulsive van der Waals energies. This is followed by the compound shogaol. These forces are responsible for making the interaction more stable and stronger. When the compounds interact with amino acid residues of DNA topoisomerase III beta, a number of interactions between the functional group of the compounds and amino acid of the enzyme takes place. The higher number of interactions leads to better and stronger interaction. Sometimes if the no of interactions is less, then the amount of binding energy released indicates the strength of molecular interaction between the ligands and the target enzyme.

Figures 4a and 4b depict the molecular docking interaction of Di with the proposed cancer target. From the figure, it is evident that dillapiole (Di) is docked into the active site of the enzyme and is making hydrogen bonding with Valine 529 of the enzyme. Valine is a non-polar amino acid and it resides in the interior groove of the enzyme. Similarly, ellagic acid (Ea) docks with the enzyme topoisomerase III beta with six hydrogen bonding interactions shown in Figs. 5a and 5b. The amino acids which interact with Ea are Ser 443, Glu 465, Glu 465, Leu 255, Leu 256, and Val 529. Glutamic acid being an acidic amino acid residue on the surface of the enzyme and the others are non-

Table 4. Binding Energies of Top Ten Binding Modes of Small Dietary Phytochemical-cancer Target-DNA Topoisomerase (Beta III) Complex with Standard Anticancer Drugs During Molecular Docking Procedure

Small phytochemical	Global energy (Total binding energy) of top ten binding interactions (Solution No/docking mode) in kcal mol^{-1} Different solutions represent different docking modes between protein and ligand									
	1	2	3	4	5	6	7	8	9	10
Di	-32.36	-27.27	-27.58	-16.78	-28.47	-28.12	-17.42	-25.63	-22.14	-18.06
Ea	-20.21	-33.44	-36.71	-30.23	-30.50	-29.87	-31.73	-15.34	-17.11	-26.52
Fe	-23.25	-26.25	-19.19	-41.25	96.99	-39.35	-23.94	-5.47	-26.25	-13.07
Sh	-36.16	-19.86	-6.36	-21.01	-8.38	-10.35	-33.85	-22.27	-28.92	-12.40
Cr	-35.14	-28.48	202.88	-42.43	-35.29	-37.27	-33.84	-40.10	-33.30	-45.84
Standard drugs azacytidine (Breast cancer)	-12.46	-14.22	-34.08	-8.73	-14.31	-30.54	-30.18	-31.02	-26.34	-25.86
Afinator (Lung cancer)	74.91	-43.49	-28.09	9.86	-44.12	-22.67	-26.14	-6.69	-5.54	9.61

Table 5. Different Types of Interaction with their Energy Release between Potential Food Phytochemicals and Cancer Target DNA Topoisomerase Beta III

Dietary phytochemical	Highest global energy/Binding energy (kcal mol^{-1})	Attractive van der waals force (kcal mol^{-1})	Repulsive van der waals force (kcal mol^{-1})	Atomic contact energy (Solvation free energy) (kcal mol^{-1})	Amino acid involved in hydrogen bonding interaction	Predicted hydrogen bond length (A)
Di	-32.36	-14.74	2.22	-7.75	Val 529	1.5313
					Ser 443	2.4815
					Glu 465	2.7489
					Glu 465	3.0655
					Leu 255	3.4547
					Leu 256	3.2054
Ea	-36.71	-18.18	1.10	-6.82	Val 529	3.0784
Fe	-26.43	-11.30	2.86	-7.93	Gln201	3.0302
					Asp77	2.3828
Sh	-36.16	-18.52	5.22	-8.71	Glu 530	3.3665
					Val 338	2.2338
Cr	-42.43	-20.05	4.32	-12.87	Val338	2.6634

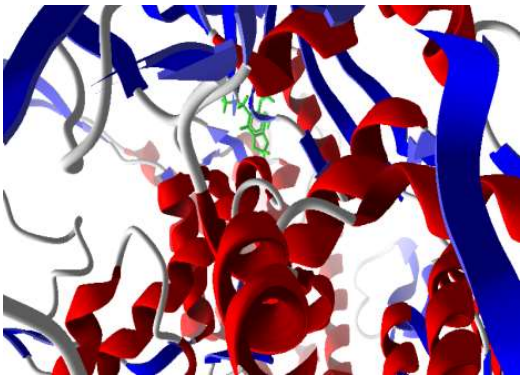

a

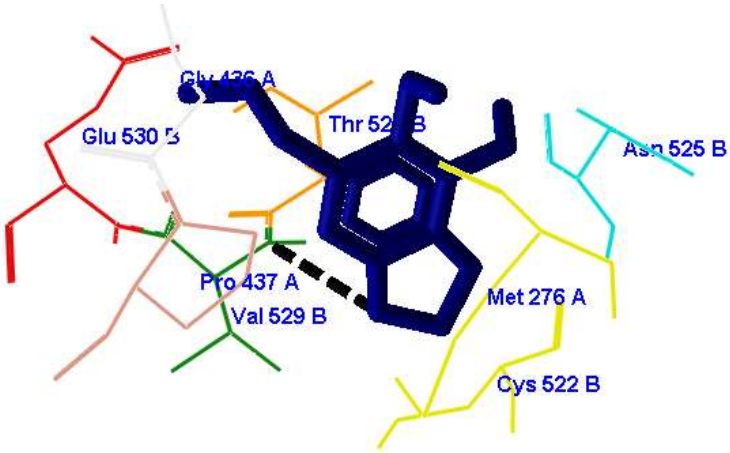

b

Fig. 4. a) Bioactive compound-Di (fluorescent green) is shown docked into the groove of the cancer target enzyme shown in tertiary structure-alpha helix (red) and beta pleated sheet (blue). b) Molecular docking showing the interaction between dietary bioactive compound-Di (Blue) with amino acid-Val 529 (green) of the target enzyme (DNA topoisomerase III beta-5GVC).

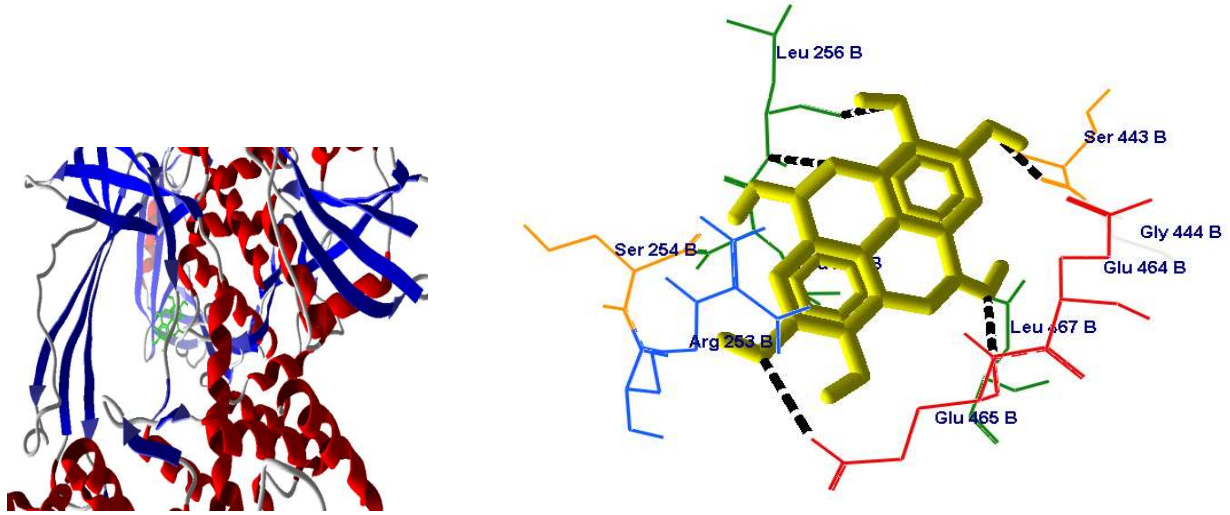

a b

Fig. 5. a) Bioactive compound-Ea (fluorescent green) is shown docked into the groove of the cancer target enzyme shown in tertiary structure-alpha helix (red) and beta pleated sheet (blue). b) Molecular docking showing the interaction between food bioactive compound-Ea (Yellow) with amino acid- Ser 443 (orange), Glu 465 (red), Glu 465 (red), Leu 255 (green), Leu 256 (green), Val 529 (not shown) of the target enzyme (DNA topoisomerase III beta-5GVC).

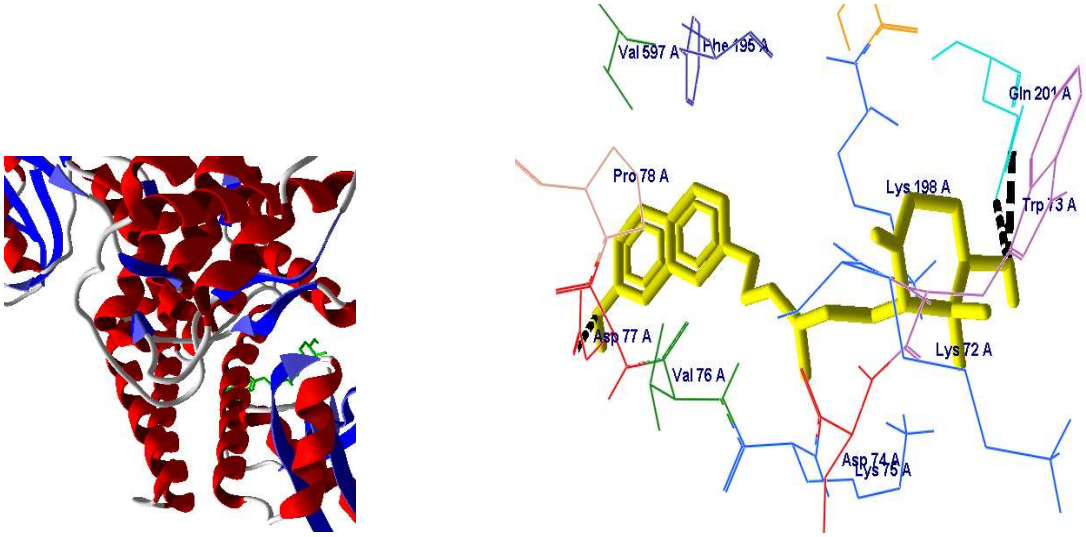

a b

Fig. 6. a) Bioactive compound-Fe (fluorescent green) is shown docked into the groove of the cancer target enzyme shown in tertiary structure- alpha helix (red) and beta pleated sheet (blue). b) Molecular docking showing interaction between dietary bioactive compound-Fe (Maroon) with amino acid-Val 529 (Green) of the target enzyme (DNA topoisomerase III beta-5GVC).

polar amino acids. It indicates that the compound has the ability to interact with both the polar and non-polar amino acids of the cancer target. The docking interaction of the third phytochemical namely fernesiferol (Fe) is shown in Fig. 6a and Fig. 6b. It depicts hydrogen bonding interactions with amino acids Gln 201and Asp 77 of the target enzyme. Shogaol (Sh) is another bioactive compound for docking, reveals the presence of five hydrogen bonding with amino

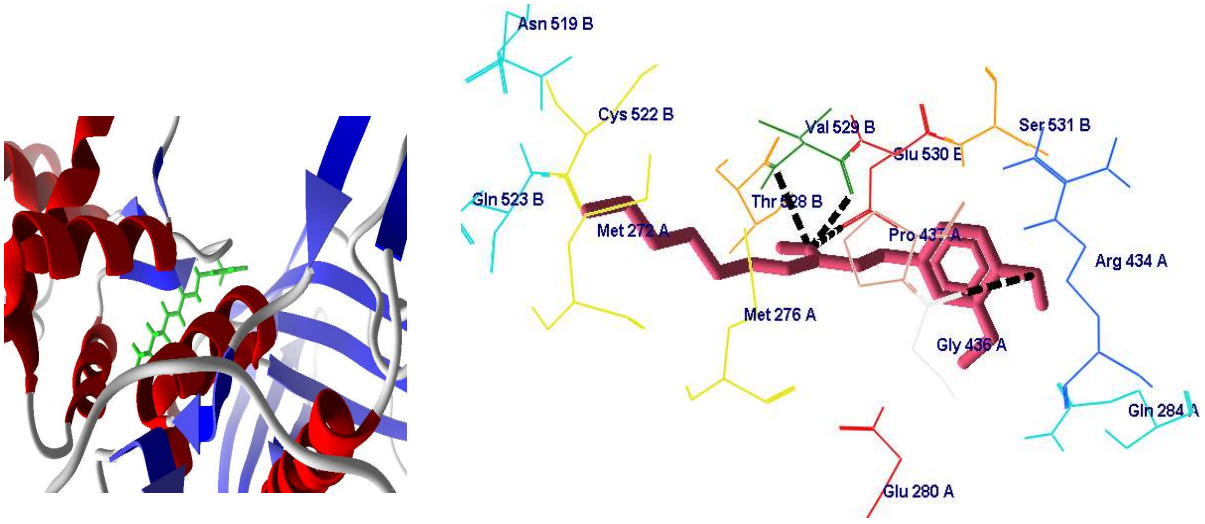

a **b**

Fig. 7. a) Bioactive compound-Sh (fluorescent green) is shown docked into the groove of the cancer target enzyme shown in tertiary structure-alpha helix (red) and beta pleated sheet (blue). b) Molecular docking showing the interaction between food bioactive compound-Sh (Pink) with amino acid- Gly 436 (white), Val 529 (green), Val 529 (green), Glu 530 (red), Leu 256 (green) of the target enzyme (DNA topoisomerase III beta-5GVC).

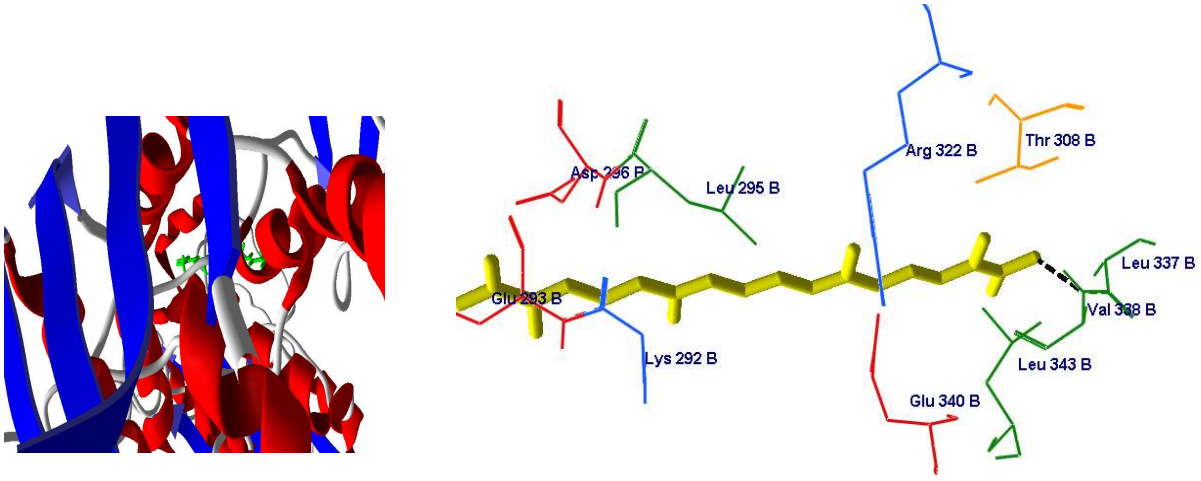

a **b**

Fig. 8. a) Bioactive compound-Cr (fluorescent green) is shown docked into the groove of the cancer target enzyme shown in tertiary structure-alpha helix (red) and beta pleated sheet (blue). b) Molecular docking showing the interaction between food bioactive compound-Cr (Yellow) with amino acid-Val 338 (green) of the target enzyme (DNA topoisomerase III beta-5GVC).

acids namely Gly 436, Val 529, Glu 530, Leu 256, and Val 529. The binding modes during docking of Sh are presented in Figs. 7a and 7b. Crocetin (Cr) is interacting with just one hydrogen bonding with Val 338 of DNA topoisomerase III beta whose docking interaction is shown in Figs. 8a and 8b. The studied dietary phytochemicals were also contributing towards various non-bonding interactions such as alkyl, pi alkyl, pi sigma, pi lone pair, and carbon-hydrogen with

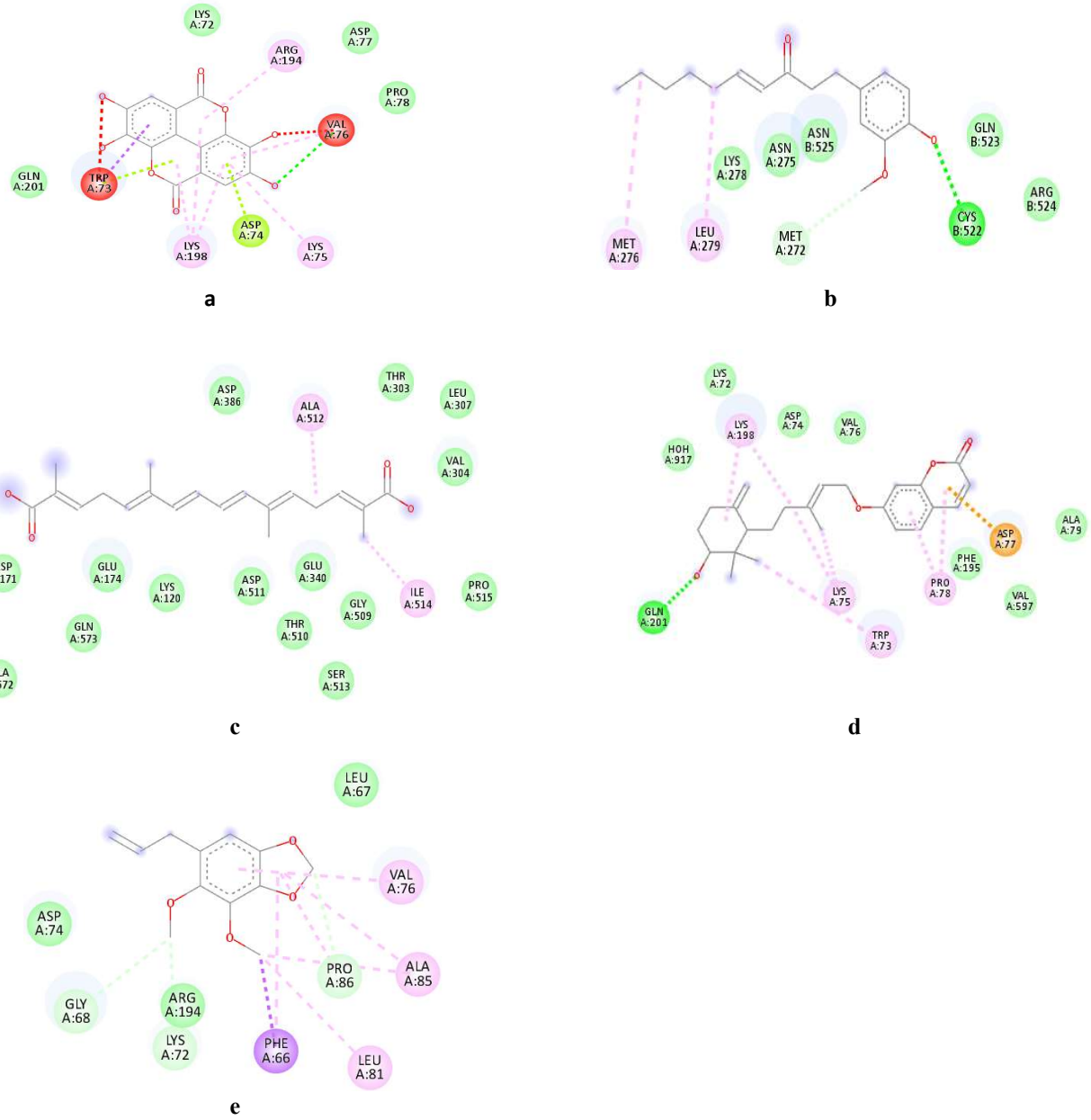

Fig. 9. a) Ea (centre) is showing pi sigma bond with Arg 194, Pi lone pair interaction with Asp 74, and Trp 73 of the protein b) Sh (centre) is showing alkyl bond with Met 276, Leu 279, and carbon-hydrogen bond with Met 272. c) Cr (centre) is making alkyl interaction with Ile 514, Ala 512. d) Fe (centre) is making alkyl interaction with Lys 75 and Lys 198, pi alkyl interaction with Lys 198 and Pro78, pi anion interaction with Asp 77. e) Di (centre) is making carbon-hydrogen bond with Pro 86, alkyl bond with Leu 81, Pi alkyl bond with Val 76, Ala 85, Phe 86, Pro 86, Pi sigma bond with Phe 66.

specific amino acid residues of the cancer target. Visualization of the non-bonding interactions is performed using the Discovery studio molecular docking visualizer. These unusual types of interactions clearly indicate the way in which the binding site of the target and the corresponding amino acid interact with each other. All these non-bonding interactions were shown in Figs. 9a, 9b, 9c, 9d, and 9e.

The molecular docking study revealed that, out of the five

compounds chosen for investigation, ellagic acid and shogaol are the compounds that make stronger interactions with the cancer target. The general notion is that the stronger the interaction, the higher will be the released binding energy. However, a binding energy study from molecular docking experiment revealed that it is not always necessary. As in the case of crocetin with just one hydrogen bonding, it exhibits binding energy of -42.43 kcal mol^{-1}. The next higher binding energy is displayed by fernesiferol, elagic acid and shogaol with values, -41.25 kcal mol^{-1}, -36.71 kcal mol^{-1} and -36.16 kcal mol^{-1} respectively. The probable reason for this kind of anomaly would be the difference in their chemical structure which can alter their biophysical interaction [31-33]. Thus to understand more of the interaction in these compounds, density functional theory analysis has also been performed. The stability and reactivity of these compounds are studied in the light of conceptual density functional theory by computing various global reactivity parameters. The DFT results and the molecular docking results are well connected with each other. The binding study indicates that it is the hydroxyl group (OH) present in these phytochemicals, that plays an important role in interacting with different functional groups *e.g.* (-C=O, -OH, -NH) of the enzymes. Various hydrogen bonding interactions between the compounds and DNA topoisomerase III beta have been listed in Table 6. Also, various non-bonding interactions between them were shown in Table 7. The amino acid involved in these interactions were shown in Figs. 9 a, b, c, d, and e.

The results of binding modes of two FDA-approved drugs Afinator and Azacitidine against DNA topoisomerase III beta are shown in Table 8. The amount of binding energy released for Afinator and Azacitidine was found to be -44.12 kcal mol^{-1} and -34.08 kcal mol^{-1}, respectively. From the molecular docking results of the five small dietary phytochemicals shown in Table 5, we found that crocetin (-42.43 kcal mol^{-1}), fernesiferol (-41.25 kcal mol^{-1}), ellagic acid (-36.71 kcal mol^{-1}), and shogaol (-36.1 kcal mol^{-1}) have more binding energy than the FDA approved Azacitidine.. Even crocetin (-42.43 kcal mol^{-1}) is showing almost comparable binding affinities as that of the second FDA-approved drug Afinator. The docking interaction of Azacitidine and Afinator is shown in Figs. 10a and 10b, respectively. The results reveal that Azacitidine interacts through four hydrogen bonds with amino acids Trp 73, Glu 268, Asp 65, and Val 76 while Afinator is involved in five hydrogen bonding interactions with amino acids Asp 65, Thr 63, Glu 268, Asp 266, and Arg 18.

CONCLUSIONS

Five potential dietary phytochemicals *e.g.* crocetin (Cr),

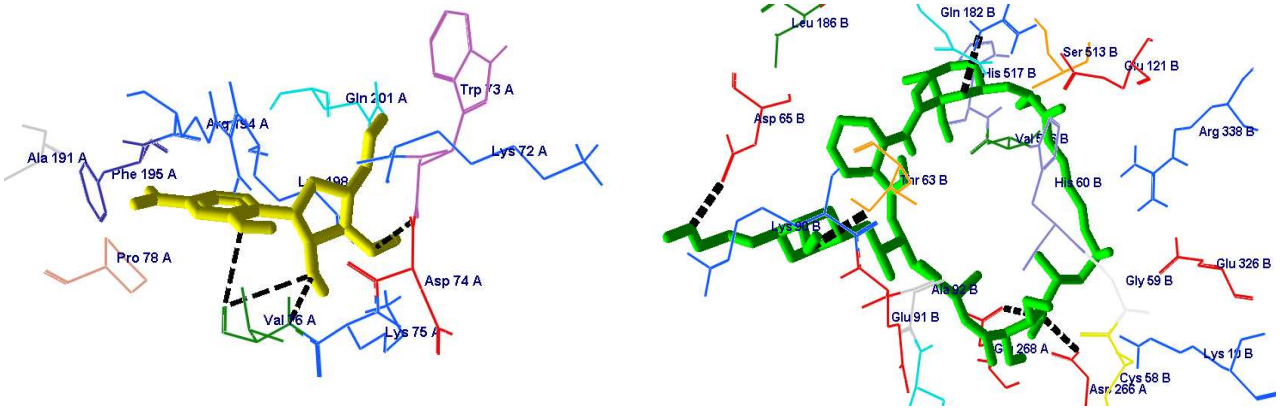

a **b**

Fig. 10. a) Molecular docking showing the interaction between FDA-approved cancer drug -Azacitidine (Yellow) with amino acid- Trp 73 (purple) and Val 76 (green) of the target enzyme (DNA topoisomerase III beta-5GVC). b) Molecular docking showing the interaction between second FDA-approved cancer drug-Afinator (fluorescent green) with amino acid- asp 65 (red), thr 63 (orange), glu268 (red), Asp 266 (red), Arg 181 (blue) of the target enzyme (DNA Topoisomerase III beta-5GVC.

Table 6. Type of Molecular Interaction between Cancer Target and the Bioactive Compounds

Bioactive compounds	Types of hydrogen bonding between bioactive compound- DNA Topo III beta complex
Di	-O-H----O=C-
	-O-H----O=C-
	-O-H----H-O-
Ea	-O----H-N-
Fe	-O-H---N-H
	-O-H---O=C-
	-O-H---H-O-
Sh	-O-H----N-H-
Cr	-O-H---N-H-

Table 7. Different Types of Non-bonding Interaction between Dietary Phytochemicals and DNA Topoisomerase III Beta

Compounds	Types of non-bonding interactions
Di	Alkyl, pi alkyl, pi sigma
Ea	pi sigma, pi lone pair
Fe	Alkyl, pi alkyl, pi anion
Sh	Alkyl, carbon hydrogen
Cr	Alkyl

Table 8. Different Types of Interaction with their Energy Release between Potential FDA Approved Cancer Drugs and Cancer Target DNA Topoisomerase III Beta

Standard drugs	Highest global energy/Binding energy (kcal mol^{-1})	Attractive van der waals energy (kcal mol^{-1})	Repulsive van der waals energy (kcal mol^{-1})	Atomic contact energy (Solvation free energy (kcal mol^{-1})	Amino acid involved in interaction	No of interaction (Hydrogen bonding)
Azacytidine (Breast cancer)	-34.08	-12.91	1.06	-10.00	Trp 73, Val 76 Glu 268, Asp	4
Afinator (Lung cancer)	-44.12	-34.61	19.54	-5.32	65, Thr 63, Asp 266, Arg 181	5

ellagic acid (Ea), fernesiferol (Fe), dillapiole (Di), and Shogaol (Sh) have been investigated thoroughly using various computational approaches. DFT calculations recognized all the compounds as stable structures. The computed quantum chemical descriptors indicate their chemical stability and reactivity. The molecular electrostatic

potential (MEP) predicts the sites of electrophilic and nucleophilic interaction in these compounds. The region near the oxygen atoms with high electron density is predicted to be the site for electrophilic reactivity. While the regions near the hydrogen atoms are the sites for nucleophilic reactivity of these phytochemicals. Molecular docking results conclude that all these natural phytochemicals have the binding ability with the cancer target-DNA topoisomerase III beta. Among the five studied bioactive molecules, Ea, Sh, Fe and Cr have higher binding energy compared to FDA approved drug azacitidine. Cr is found to have the highest binding energy of -42.43 kcal mol^{-1} which is comparable with another FDA-approved drug afinator. The linear structure of crocetin allows the molecule to interact strongly with the amino acid residues of the enzyme. The results of DFT analysis revealed Cr as the most reactive molecule with the lowest ionization potential which is supported by the highest binding energy of Cr in the molecular docking study. Thus, our DFT results are in sync with the molecular docking studies.

Anticancer synthetic drugs are of high molecular weight and they exhibit tremendous side effects. In this context, our studies with low molecular weight natural phytochemicals can be thought of as an option for replacing high molecular weight synthetic drugs. Therefore, Cr along with Fe, Ea and Sh, it has high potential to act as an anticancer drug. However, this work has to be substantiated with biological laboratory-based experiment.

ACKNOWLEDGEMENTS

The authors are highly grateful to Sharda University, Greater Noida, for providing Gaussian 16 for the DFT calculations to accomplish this study.

REFERENCES

[1] Hornyak, P.; Askwith, T.; Walker, S.; Komulainen, E.; Paradowski, M.; Pennicott, L. E., Mode of action of DNA-competitive Small Molecule Inhibitors of Tyrosyl DNA Phosphodiesterase 2. *Biochem. J.* **2016**, *473*, 1869-79. DOI: 10.1042/BCJ20160180.

[2] Nitiss, J. L., Targeting DNA TopoisomeraseIIincancerchemotherapy. *Nat. Rev. Cancer.* **2009**, *9*, 338-50. DOI: 10.1038/nrc2607.

[3] Gore, M.; Desai, N. S., Computer-aided drug Designing. *Methods Mol. Biol.* **2014**, *1168*, 313-321. DOI: 10.1007/978-1-4939-0847-9_18.

[4] Hanee, U.; Rahman, M. R.; Matin, M. M., Synthesis, PASS, *In Silico* ADMET, and Thermodynamic Studies of some Galactopyranoside Esters. *Phys. Chem. Res.*, **2021**, *9*(4), 591-603. https://doi.org/10.22036/pcr.2021.282956.1911

[5] Muhammad, D.; Matin, M. M.; Miah, S. M. R.; Devi, P., Synthesis, antimicrobial, and DFT Studies of some Benzyl 4-O-acyl-α-L-rhamnopyranosides. *Orbital: The Electronic Journal of Chemistry*, **2021**, *13*(3), 250-258. http://dx.doi.org/10.17807/orbital.v13i3.1614.

[6] Meng, X. Y.; Zhang, H. X.; Mezei, M.; Cui, M., Molecular Docking: A Powerful Approach for Structure-based Drug Discovery. *Curr Comput Aided Drug Des.* **2011**, *7*(2), 146-157. DOI: 10.2174/157340911795677602.

[7] Duhovny, D. S.; Inbar, Y.; Nussinov, R.; Wolfson, H. J., PatchDock and SymmDock: Servers for Rigid and Symmetric Docking. *Nucleic Acids Res.* **2005**, *33*, 363-367. https://doi.org/10.1093/nar/gki481.

[8] Pinzi L., Ratelli G., Molecular Docking: Shifting Paradigms in Drug Discovery. *Int. J. Mol. Sci.* **2019**. *20*, 18, 4331. DOI: 10.3390/ijms20184331.

[9] Hashemi, A.; Bathaie, Z.; Mohagheghi, M. A.; Crocetin and Crocin Decreased Cholesterol and Triglyceride Content of both Breast Cancer Tumors and Cell Lines. *Avicenna J. Phytomedicine.* **2020**. *10*(4), 384-397. PMCID: PMC7430959.

[10] Miriam, R.; Jonah, E.; David, E. Z.; Carrell, H. L.; Brend, I., The Crystal and Molecular Structure of Ellagic Acid Dihydrate: A Dietary Anti-cancer Agent. *Carcinogenesis*. **1991**, *12*(12), 2227-2232. https://doi.org/10.1093/carcin/12.12.2227.

[11] Mao, Z. W.; Jin, G.; Yang, C.; Jie, N.; Ming, C.; Qiang, S.; Li, H. P.; Zhi, H. J., Synthesis of Crocetin Derivatives and their Potent Inhibition in Multiple Tumor Cells Proliferation and Inflammatory Property of Macrophage. *BMC Complement Altern. Med.* **2020**, *20*, 29. doi.org/10.1186/s12906-020-2831-y.

[12] Flores-Holguin, N.; Frau, J.; Glossman-Mitnik,D. Chemical Reactivity and Bioactivity Properties of the Phalotoxin Family of Fungal Peptides Based on

Conceptual Peptidology and DFT Study. *Heliyon*. **2019**, *5*, e02325. https://doi.org/10.1016/j.heliyon.2019.e02335.

[13] Eryilmaz, S.; Gul, M.; Inkaya, E., Investigation of Global Reactivity Descriptors of some Perillaldehyde Derivatives in Different Solvents by DFT Method. *Indian J. Chem. Technol.* **2019**, *26*, 235-238. http://nopr.niscpr.res.in/handle/123456789/48465.

[14] Sibuh, B. Z.; Khanna, S.; Taneja, P.; Sarkar, P.; Taneja, N. K., Molecular Docking, Synthesis and Anticancer Activity of Thiosemicarbazone Derivatives against MCF-7 Human Breast Cancer Cell Line. *Life Sci.* **2021**, *273*, 119305. https://doi.org/10.1016/j.lfs.2021.119305.

[15] Waterbeemd, H. V.; Gifford, E., ADMET *In Silico* Modelling: Towards Prediction Paradise. *Nat. Rev.* 2003, *192*(2), 192-204. DOI: 10.1038/nrd1032.

[16] Frisch, M. J.; Trucks, G. W.; Schlegel, H. B.; Scuseria, G. E.; Robb, M. A..; Cheeseman, J. R.; Scalmani, G.; Barone, V.; Petersson, G. A.; Nakatsuji, H.; Li, X.; Caricato, M.; Marenich, A. V.; Bloino, J.; Gomperts, B.; Mennucci, H. P.; Hratchian, J. V.; Ortiz, A. F.; Izmaylov, J. L.; Sonnenberg, D.; Williams-Young, F.; Ding, F.; Lipparini, F.; Egidi, J.; Goings, B.; Peng, A.; Petrone, T.; Henderson, D.; Ranasinghe, V. G.; Zakrzewski, J.; Gao, N.; Rega, G.; Zheng, W.; Liang, M.; Hada, M; Ehara, K.; Toyota, R.; Fukuda, J.; Hasegawa, M.; Ishida, T.; Nakajima, Y.; Honda, O.; Kitao, H.; Nakai, T.; Vreven, K.;Throssell, J. A.; Montgomery, Jr.; Peralta, J. E.; F. Ogliaro, M. J.; Bearpark, J. J.; Heyd, E. N.; Brothers, K. N.; Kudin, V. N.; Staroverov, T. A.; Keith, R.; Kobayashi, J.; Normand, K.; Raghavachari, A. P.; Rendell, J. C.; Burant, S. S.; Iyengar, J.; Tomasi, M.; Cossi, J. M.; Millam, M.; Klene, C.; Adamo, R.;Cammi, J. W.; Ochterski, R. L.; Martin, K.; Morokuma, O.; Farkas, J. B.; Foresman, D. J., Fox,' Gaussian, Inc. Wallingford CT, **2016**.

[17] Ravikumar, C.; Murugavel, S.; Guin, M.; Silambarasan, T., Crystal Structure, Hirshfeld, Computational Biomolecular Investigations, and MTT Assay Studies of Amino Pyrimidine Derivative as EGFR Kinase Domain Inhibitor. *J. Mol. Struct.* **2022**, *1254*, 132416. https://doi.org/10.1016/j.molstruc.2022.132416.

[18] Guin, M.; Verma, V. K.; Singh, R.; Singh, R. C., Molecular Structure and HOMO/LUMO Analysis of 1,1'-Spirobi[3H-2,1-benzoxaselenolene] by Quantum chemical investigation. *Macromol. Symp.* **2021**. https://10.1002/masy.202000252.

[19] Verma, V.K.; Guin, M..; Solanki, B.; Singh, R.C. Molecular Structure, HOMO and LUMO Studies of Di(Hydroxybenzyl)diselenide by Quantum Chemical Investigations. *Mater. Today: Proc.* **2020**, *49*, 3200-3204. https://doi.org/10.1016/j.matpr.2020.11.887.

[20] Calsteren, M. -R. V.; Bissonnette, M. C.; Cormier, F.; Dufresne, C.; Ichi, T.; LeBlanc, J. C. Y.; Perreault, D.; Roewer, I., Spectroscopic Characterization of Crocetin Derivatives from Crocussativus and Gardenia jasminoides. *J. Agric. Food Chem.* **1997**, *45*, 1055-1061. https://doi.org/10.1021/jf9603487.

[21] Goriparti, S.; Harish, M. N. K.; Sampath, S., Ellagic acid-A Novel Organic Electrode Material for High Capacity Lithium Ion Batteries. *Chem. Commun.* **2013**, *49*, 7234-7236. DOI: https://doi.org/10.1039/C3CC43194K.

[22] Hassan, S.; Hamed, S.; Almuhayawi, M.; Hozzin, W.; Selim, S.; AbdElgawad, H., Bioactivity of Ellagic Acid and Velutin: Two Phenolic Compounds Isolated from Marine Algae. *Egypt. J. Bot.*, **2021**, *61*(1), 219-231. DOI: 10.21608/ejbo.2020.23778.1456.

[23] Kasaian, J.; Mohammadi, A., Biological Activities of farnesiferol C: A review. *Journal of Asian Natural Products Research*, **2018**, *20*(1), 27-35. DOI: 10.1080/10286020.2017.1379997.

[24] Ferreira, R. G.; Monteiro, M. C.; da Silva, J. K. R.; Maia, J. G. S., Antifungal Action of the Dillapiole-rich Oil of Piper Aduncum Against Dermatomycoses Caused by Filamentous Fungi. *British Journal of Medicine & Medical Research*, **2016**, *15*(12), 1-10. DOI: 10.9734/BJMMR/2016/26340.

[25] Rojas-Martínez, R.; Arrieta, J.; Cruz-Antonio, L.; Arrieta-Baez, D.; Velázquez-Méndez A. M.; Sánchez-Mendoza, M. E., Dillapiole, Isolated from Peperomia pellucida, Shows Gastroprotector Activity against Ethanol-Induced Gastric Lesions in Wistar Rats. *Molecules*, **2013**, *18*, 11327-11337. DOI: 10.3390/molecules180911327.

[26] Seow, S. L. S.; Hong, S. L.; Lee, G. S.; Malek, S. N. A.; Sabaratnam, V., 6-Shogaol, a Neuroactive Compound

of Ginger (Jahe Gajah) Induced Neuritogenic Activity *via* NGF Responsive Pathways in PC-12 Cells, *BMC Complementary and Alternative Medicine*, **2017**, *17*, 334. DOI: 10.1186/s12906-017-1837-6.

[27] Pearson, R. G., Absolute Electronegativity and Absolute Hardness of Lewis Acids and Bases. *J. Am. Chem. Soc.* **1985**, *107*(24), 6801-6. https://doi.org/10.1021/ja00310a009.

[28] Xavier, S.; Periandy, S., Spectroscopic (FT-IR, FT-Raman, UV and NMR) Investigation on 1-Phenyl-2-Nitropropene by Quantum Computationalcalculations. *Spectrochim. Acta A.* **2015**. *149*, 216-230. 10.1016/j.saa.2015.04.055.

[29] Susan, A. C.; Christian P.; Muthu, S., Quantummechanical, Spectroscopic and Docking Studies of 2-Amino-3-bromo-5-nitropyridine by Density Functional Methods. *Spectrochim. Acta A*, **2017**, *181*, 153-163. DOI: 10.1016/j.saa.2017.03.045.

[30] Reed, A. E.; Weinhold, F., Natural Localized Molecular Orbitals. *Chem. Phys.* **1985**, *83*, 1736-1740. https://doi.org/10.1063/1.449360.

[31] Oussama, C.; Abbdellah, E. L.; Youssef, E. O.; Bouachrine, M.; Ouammou, A., *In Silico* Prediction of Novel (TRIM24) Bromodomain Inhibitors: A Combination of 3D-QSAR, Molecular Docking, ADMET Prediction, and Molecular Dynamics Simulation. *Phys. Chem. Res*., **2022**, *10*(4), 519-535. DOI: 10.22036/PCR.2022.331866.2040.

[32] Kasmi, R.; Bouachrine, M.; Ouammou, A., Combined 3D-QSAR and Molecular Docking Analysis of Styrylquinoline Derivatives as Potent anti-cancer Agents. *Phys. Chem. Res.*, **2022**, *10*(3), 345-362. DOI: 10.22036/PCR.2021.304969.1967.

[33] Khatabi, K. El.; El-mernissi, R.; Aanouz, I.; Ajana, M. A.; Lakhlifi, T.; Shahinozzaman, M.; Bouchrine, M., Benzimidazole Derivatives in Identifying Novel Acetylcholinesterase Inhibitors: A Combination of 3D-QSAR, Docking and Molecular Dynamics Simulation. *Phys. Chem. Res*., **2022**, *10*(2), 237-249. DOI: 10.22036/PCR.2021.277306.1895.